Supplemental Materials to

Aβ oligomers induce synaptic damage via Tau dependent microtubule severing by TTLL6 and spastin

Running Title: Aβ causes microtubule severing by spastin via Tau

Hans Zempel[1], Julia Luedtke[1,2], Yatender Kumar[1,2], Jacek Biernat[1], Hana Dawson[4], Eckhard Mandelkow[1,2,3], Eva-Maria Mandelkow[1,2,3]

[1]DZNE, German Center for Neurodegenerative Diseases, Bonn, Germany
[2]MPI for Neurological Research, Hamburg Outstation, Hamburg, Germany
[3]CAESAR Research Center, Bonn, Germany
[4]Duke University Medical Center, Durham, NC, USA

Supplemental Results

(a) Oligomers of Aβ are most potent and synaptotoxic in the pathological ratio as present in AD brains

Aβ deposition is a major hallmark of the progression of AD and may be a causative factor. Recently, oligomeric forms of Aβ have been identified as the primary toxic species in AD (Benilova et al, 2012). To be able to investigate the Aβ induced changes on Tau and the neuronal cytoskeleton, we first screened several oligomeric preparations of Aβ for their influence on Tau localization and synaptotoxicity in sub-lethal concentrations. In order to prevent non-specific side-effects of Aβ oligomer preparations, we decided to use only preparations without cell culture medium, since all cell culture media contain amino acids that are active in neuronal signalling. For continuity and comparability to previous studies (Klein et al, 2004; Zempel et al, 2010), we used a modified version of a previously used Aβ preparation (ADDLs; Aβ Derived Diffusible Ligands), modified ADDLs (mADDLs), which consists of $Aβ_{1\text{-}42}$ and still contains DMSO, but no cell culture medium (see methods). We also tested oligomeric preparations of $Aβ_{1\text{-}42}$ without DMSO, $Aβ_{1\text{-}40}$ without DMSO, and a mixture of $Aβ_{1\text{-}40}$ and $Aβ_{1\text{-}42}$ in the pathological ratio as present in AD brains (Kuperstein et al, 2010), i.e. in the ratio of 7 parts $Aβ_{1\text{-}40}$ and 3 parts $Aβ_{1\text{-}42}$ (termed $Aβ_{7:3}$). As dimers might be an essential building block for fibrillar and oligomeric Abeta (Lopez del Amo et al, 2012; Walsh & Selkoe, 2007), we also used synthetically crosslinked $Aβ_{1\text{-}40}$ by isulphide bridging (O'Nuallain et al, 2010). All oligomeric forms of Aβ displayed multiple oligomeric species in SDS-PAGE, immunoreactivity with an oligomer specific antibody (A11 (Kayed et al, 2003)), and visible as heterogeneous globular structures by electron microscopy (Fig.S1). When we exposed mature primary rat hippocampal neurons to the different oligomer preparations, none of them caused overall toxic effects in terms of LDH release, and we found that all of them increased the ATP content over time (Fig.S1f,g), indicating that there is a measurable biochemical response, but no cell death at the concentrations and conditions used here. All oligomeric forms of Aβ are targeted mainly to dendritic spines (Fig. S2), as shown before (Lacor et al, 2004; Zempel & Mandelkow, 2012; Zempel et al, 2010). Also, Tau missorting and correlating spine loss could be induced with most preparations within 3h (Fig. S2a-d). However, Tau missorting, a measure of AD-like pathology in neurons (Busciglio et al, 1995), was ~3 fold higher (Fig. S2e), and spine reduction was most pronounced (Fig. S2f) with the pathological mixture of Aβ, i.e. $Aβ_{7:3}$, compared to the other Aβ oligomer preparations. We therefore decided to use $Aβ_{7:3}$ for further analysis of the effects of Aβ oligomers.

(b) Changes in MAP2 levels in the dendrites are not responsible for loss or stabilization of MTs

First, we tested whether we could detect a decrease in the microtubule associated protein 2 (MAP2), which is responsible for the stabilization of dendritic MTs. The level of dendritic MAP2 increases about 2-fold after Aβ exposure, but peaks after 3-6h and returns to baseline within 12h, sooner than missorted Tau (Fig. S6a). Since an increase of MAP2 might be a compensatory response for lost MT stability, we tested if increased expression of MAP2 prevented MT loss. Transfection of MAP2c prevented Aβ induced MT loss (Fig. S6b), but also reduced spine density, even in the absence of Aβ, possibly caused by the inhibition of motors and impaired traffic by MAP2 or suppression of MT dynamics (Hoogenraad & Bradke, 2009). As a result of spine loss, Aβ was less targeted to transfected cells. Thus MAP2 likely plays an important role in stabilizing MTs, but is not causative for the observed loss of MT after Aβ insults.

Supplemental figure legends

Figure S1: Aβ oligomers of different composition display similar oligomeric profiles in SDS-PAGE, A11 immunoreactivity and electron microscopy analysis.

(a-b) Abeta was dissolved as detailed in material and methods and 90pmol of (monomeric) protein was loaded on 5-20% gradient gels. The preparations were either kept on ice (left) or incubated at 37°C for 1h (right). Except for the synthetic dimer, all preparations contain monomers and dimers, preparations containing Abeta 1-42 also contain tri- and tetramers. Incubation results in smears of some preparations. No protein is retained in the slots. Synthetic dimers display strong signals in the dimeric and tetrameric fractions. Full gel and western blot from the slots to the dye front are shown.

(a) Unspecific reversible protein stain (zinc-imidazole).

(b) Western blot of the same gel as in a), using a polyclonal antibody against Aβ (β-amyloid AB). Despite stronger signals for e.g. in the monomeric fraction of Aβ 1-40 relativ to Aβ 1-42 in a), chemiluminescence signals for Aβ 1-40 are weaker in b), likely because of different antibody affinities.

(c) Dot blot analysis of different Aβ preparations. 300pmol were dotted on nitrocellulose membranes. Upper panel: The oligomer-specific antibody A11 recognizes all Aβ preparations independent of the incubation. Middle and lower panel: Polyclonal Aβ antibody (β-amyloid AB, middle panel) and the unspecific protein stain CPTS (lower panel) were used as loading controls.

(d) Negative stain electron microscopy of Aβ oligomer preparations. Stock solution were incubated for 1h at 37°C, diluted to 6µM in PBS medium and applied to grids. All preparations display globular particles but of different sizes and heterogeneity. Scale bars: 100nm.

(e) Magnification of outlined areas of d). Scale bars: 40nm.

(f-g) The different Aβ oligomer preparations were applied to primary rat hippocampal neurons for the indicated time at a concentration of 1µM and cytotoxicity was assayed via f) lactate dehydrogenase activity measurements in the culture medium or g) measurement of intracellular ATP after cell lysis. None of the Aβ oligomer preparations displayed cytotoxic effects, while treating cells with triton resulted in significant cell death.

Figure S2: Aβ oligomers are dendritically targeted, induce selective Tau missorting and loss of spines

Primary rat hippocampal neurons aged 21DIV were exposed for 3h to different oligomeric preparations of Aβ at a concentration of 1µM.

(a-d) The pathological ratio of Aβ (7 parts Abeta1-40, 3 parts Abeta1-42; termed $A\beta_{7:3}$ oligomers induces strong missorting and dramatic spine loss in a subset of cells (dotted boxes, magnified in (b)). Aβ oligomers are localized to dendrites that do not show strong missorting and still have spines (solid box, magnified in (c)), whereas control cells show no missorting and healthy spines d).

(e-f) Quantification of (e) missorting and (f) spine loss induced by the different oligomeric preparations after exposure to 1µM Aβ oligomers for 3h. $A\beta_{7:3}$ oligomers induced most pronounced missorting and spine reduction.

(g) In cells without Tau missorting, all types of Aβ oligomers are targeted to dendrites.

Figure S3: Overview pictures of MARK and Tau stainings for Fig. 1 (for details see Fig.1b legends)

(a) Untreated cells show only basal MARK activity and phospho-Tau staining (12E8).

(b) After treatment with AβO 1µM for 3h, pTau increases and MARK activity becomes elevated only in the soma and the dendrites. (b1) shows overview image, (b2) and (b3) show magnification of the solid and the dotted box, respectively. Arrow indicates an axon, star a cell body, and arrowhead a dendrite.

Figure S4: (a) Fast missorting of Tau induced by nocodazole or calcium does not induce elevations of KXGS-phosphorylation of Tau.
Primary rat hippocampal neurons aged 21DIV were exposed for up to 6h to nocodazole (10µM) or calcium (5mM), and stained for phosphorylation at the KXGS motifs (12E8 antibody) and pS214, both of which regulate MT affinity.
(a1) Overview images of cells. Rectangles indicate areas magnified in (a2)
(a2) Images show magnification of dendrites. Despite the appearance of Tau in dendrites (stained by total Tau antibody V20) 12E8 levels did not increase and pS214 levels remained undetectable.
(a3) Quantification as conducted for 12E8 staining in Fig. 1.
(b) Missorting of neurofilaments into the dendrites after exposure to AβO lags behind neurofilament accumulation in the cell body.
Primary rat hippocampal neurons 21DIV were treated with 1µM Aβ for different durations as indicated.
(b1) Missorting of neurofilaments is reversible: neurofilaments appear first in the soma, then in the dendrites with a delay of ~2h. Cells were fixed after different incubation lengths, and stained for neurofilaments, MAP2 for dendrite identification, and Hoechst for identification of the nucleus.
(Left panel) Control cells show very low levels of neurofilaments in the soma and dendrites.
(Middle panel) After brief treatments with Aβ (1h), neurofilaments appear in the soma (indicated by circle).
(Right panel) Later (6h), neurofilaments also appear in the dendrites (arrow).
(b2) Quantification reveals a sudden increase in neurofilaments in the cell body, and delayed increases in the proximal dendrite.

Figure S5: Katanin is not involved in AβO induced missorting of Tau and loss of MTs.
(a) Primary rat hippocampal neurons aged for 25 days were treated with 1µM AβO for 3h, fixed and stained as indicated. There is no difference in levels or distribution of katanin p80 or katanin p60 between control cells (a1) and AβO-treated cells (a2). MAP2 staining serves as a compartment marker for the soma and the dendrite.
(b-d) Knockdown experiments of katanin. Cells were transfected with a vector expressing shRNA against katanin p80 and a fluorescent marker protein to identify transfected cells (either mRFP or mTFP) for 5d.
(b) Primary neurons aged for 10days were used to show knockdown of katanin. Knockdown of katanin-p80 reduces levels of katanin-p80 but not of katanin-p60. MAP2 staining serves as a compartment marker for the soma and the dendrite. Arrows indicate transfected cell.
(c) shRNA against katanin p80 does not prevent AβO induced microtubule loss. Primary hippocampal neurons 23 DIV were transfected with shRNA against katanin p80 for 5d and treated with AβO. (Left panels) mTFP signal indicates transfected cells, arrows indicate transfected dendrite. After AβO treatment transfected cells display major loss of MTs. (Right panels) Cells transfected but left untreated displayed normal amounts of MTs.
(d) shRNA against katanin p80 does not prevent Tau missorting. (d1) Cells transfected with shRNA against katanin p80 show only normal background staining of Tau (d2) Cells transfected with shRNA against katanin p80 and treated with AβO for 3h show Tau missorting into the dendrites and soma (arrows).

Figure S6: Endogenous MAP2 increases after Aβ exposure; overexpression of MAP2c prevents AβO induced microtubule loss
Primary hippocampal neurons (21DIV) were treated with AβO (1µM) as indicated.
(a) Quantification of endogenous dendritic MAP2 increases up to ~150% after 1-6h after Aβ exposure.
(b) Neurons transfected with MAP2c tagged with Dendra2c (D2) and treated with 1µM AβO for 3h.
(b1) MAP2c transfected cells display no microtubule loss (solid box, magnified in **(b2)**), while non-transfected cells show normal decrease of MTs (dotted box, magnified in **(b3)**).

Figure S7: Silencing of spastin or Tau prevents missorting of Tau after Aβ treatment.
Primary rat hippocampal neurons (16-21DIV) were treated with 1μM Aβ for the indicated durations.
(a) Cells expressing shRNAi (RFP positive cells, dotted box, magnified in **(b)**) show reduced Tau missorting and reduced spastin levels. Neighbouring untransfected cells show Tau missorting and normal spastin levels (RFP negative cells, solid box, magnified in **(c)**).
(d) Primary rat hippocampal neurons were transfected with (d1) tdTomato alone or with (d2) tdTomato and shRNA against Tau for 20h and then treated with 1μM Aβ oligomers.
(d1) Cells normally expressing endogenous Tau show missorting of Tau into the soma and into the dendrites (arrows).
(d2) Cells transfected with shRNA against Tau for only 20h do not show missorting of Tau into the somatodendritic compartment.

Figure S8: Monomeric Aβ induces missorting of Tau in the presence of AβO after recovery.
Primary hippocampal neurons were pretreated with AβO for 21h allowing them to recover, and then treated with different species of monomeric, dimeric or oligomeric Aβ as indicated for an additional 3h, fixed and stained as indicated.
(a) Quantification of the percentage of missorting after pretreatment with AβO and recovery. Missorting is strongly enhanced in the presence of AβO after recovery in the case of monomeric Aβ1-42, slightly enhanced for monomeric mixed Aβ (7 parts Aβ1-40, 3 parts Aβ1-42) and the synthetic dimer, and not enhanced in case of monomeric Aβ1-40 alone.
(b-d) representative images of
(b) untreated control cells not displaying missorting,
(c) cells treated for 21h with AβO (allowing recovery) and then treated with monomeric Aβ1-42, resulting in missorting into the soma and the dendrite (arrows),
(d) cells treated only with monomeric Aβ1-42, not showing missorting.

Figure S9: Inhibition of MARK does not result in missorting of Tau
Primary rat hippocampal neurons 24DIV were treated with 1μM of the specific MARK Inhibitor compound 39621 or with 1μM AβO for 3h, fixed and stained as indicated.
(a) Control cells show no Tau in the dendrites (no overlay with the dendritic marker MAP2) and only background staining in the cell body.
(b) Inhibition of MARK does not result in missorting of Tau.
(c) AβO treatment induces missorting of Tau in the dendrites and the soma (arrows).

Figure S10: Spontaneous calcium oscillations recover in neurons from TauKO, but not from wildtype mice 24h after exposure to Aβ.
Spontaneous calcium oscillations of high density primary cortical neurons 19-20DIV visualized fluorimetrically with Fluo4/F127.
(a) Different excitation states of the same cells either at (A) the lowest Ca^{++} levels (~100nM), or (B) medium calcium levels (~300nM) attainable spontaneously, or (C) at high Ca^{++} levels (~1μM) after addition of high glutamate (1mM final concentration).
(b) Fluorescence measurement of the above cell. **(c)** Fluorescence measurements of wildtype (black graphs) and TauKO (red graphs) without (upper panels) or with Aβ treatment (lower panels) for 24h. The spontaneous Ca^{++} dynamics of wildtype, but not of TauKO cells remains impaired after 24h.
(d) Quantification of (c).

Figure S11: (a) Wildtype primary neurons from mice recapitulate the same phenotypes as neurons from rats: Tau missorting, calcium elevations and spine loss after treatment with Aβ or glutamate.
Primary mouse hippocampal neurons 19-20DIV were treated with AβO (1μM) or glutamate (10μM) and stained as indicated. Treatments result in Tau missorting into the somatodendritic compartment, and in corresponding loss of spines (upper panel) or Ca^{++} elevations (lower panel).
(b,c) Reintroduction of KXGE-Tau, but not of KXGA-Tau, re-establishes loss of spines and reduction of AβO association with dendrites after exposure to AβOS.

Primary hippocampal neurons from TauKO mice were transfected for 3 days with CFP-tagged human Tau (hTau40) mutated at the KXGS motifs, either to KXGA (preventing phosphorylation), or to KXGE (mimicking phosphorylation) and treated with AβO for 3h. Cells were fixed and stained for spines and Aβ.
(b1) Transfection with KXGE-Tau re-establishes Aβ-induced loss of spines and the concomitant prevention of Aβ accumulation (magnified box in b2).
(c1) KXGA-Tau does not enhance spine loss nor abolishes association of AβO with dendrites (magnified box in c2).
(d) Re-introduction of KXGE-Tau, but not KXGA-Tau re-establishes loss of MTs, calcium elevations and mitochondrial clustering in the soma after exposure to AβO.
Primary hippocampal neurons from TauKO mice were transfected via Adenovirus for 3d with CFP-hTau40 mutated at the repeat domain to either KXGE or KXGA and treated with AβO (1µM, 3h) and stained as indicated.
(Upper panel) KXGE-Tau transfected cells display loss of MTs, elevated Ca^{++} and clustering of mitochondria.
(Lower panel) KXGA-Tau transfected cells show normal levels (similar to TauKO cells) of MTs and Ca^{++}, and evenly distributed mitochondria.

Figure S12: Overview pictures of Tau, MAP2, polyglutamylated microtubules and TTLL6 stainings for Fig.3a (for details see Fig.3a legends)
Primary rat hippocampal neurons 21DIV treated with 1µM Aβ for 3h. MAP2 was used as a marker for the somatodendritic compartment.
(a) Overview pictures of Fig.3a1 and Fig.3a2. Magnified dendrites in Fig.3a were cropped out of the regions marked by dotted boxes. Solid boxes are magnified in (b).
(b) Magnification of solid boxes of a. Magnifications show only axons: They are positive for Tau (upper left panels; green color), but devoid of MAP2 (lower left panels; blue color). There is no change in polyglutamylation of microtubules or TTLL6 in axons (right panels) of Aβ treated cells **(b2)** compared to controls **(b1)**.

Supplemental table 1: Antibodies and labeling reagents used in this study

Protein/Structure (clone/reagent name)	*dilution*	*host-species*	*company*
Tau (K9JA)	1:500 1:5000 (WB)	rabbit	Dako
pTau (12E8)	1:200 1:2000 (WB)	mouse	Elan
F-actin (CF405-Phalloidin)	1:50	n.a.	Biotium
F-actin (Rhodamin-Phalloidin)	1:100	n.a.	Cytoskeleton
pMark/active MARK (pT208)	1:200	rabbit	Eurogentec
total MARK (SA4635)	1:750 (WB)	rabbit	Eurogentec
Nucleus (Hoechst)	1:2000	n.a.	Sigma
GFP (chick. polycl.)	1:100 (IP)	chicken	Abcam
HA-Tag (rabbit. poylcl.)	1:2000 (WB)	rabbit	Sigma
Tau (V20)	1:100	goat	Santa Cruz
pTau (S214)	1:50	rabbit	Biosource
Tubulin (DM1α)	1:300 1:5000 (WB)	mouse	Sigma
tyrosinated tubulin (YL1/2)	1:1000	rat	serotec
acetylated tubulin (611B1)	1:1000 1:10000 (WB)	mouse	Sigma
polyglutamylated tubulin (B3)	1:500 1:5000 (WB)	mouse	Sigma
Spastin (Sp6C6)	1:200 1:2000 (WB)	mouse	Sigma
MAP2 (chick. polycl.)	1:10000	chicken	Abcam
MAP2 (AP20)	1:100	mouse	Sigma
mRFP (5F8)	1:200	rat	Chromotec
TTLL6 (P12)	1:200	goat	Santa Cruz
Tau (DA9)	1:100	mouse	Dr. P. Davies, AECOM
Aβ (β-amyloid AB)	1:200	rabbit	Cell signaling
neurofilament (NF200)	1:200	rabbit	Sigma
pStathmin Ser38 (D19H10)	1:1000	rabbit	Cell signaling
Kl1 (rabbit. poylcl.)	1:100	rabbit	Dr. D. Sharp, AECOM
Katanin p60 (goat polycl.)	1:50	goat	Santa Cruz
Katanin p80 (chick. polycl.)	1:300	chicken	Abcam
Rhod-2, AM	1μM	n.a.	Invitrogen
Mitotracker Deep Red, FM	50nM	n.a.	Invitrogen
Fluo-4, AM	4μM	n.a.	Invitrogen
Fura-2, AM	4μM	n.a.	Invitrogen

Supplemental References

Benilova I, Karran E, De Strooper B (2012) The toxic Abeta oligomer and Alzheimer's disease: an emperor in need of clothes. *Nature neuroscience* **15:** 349-357

Busciglio J, Lorenzo A, Yeh J, Yankner BA (1995) beta-amyloid fibrils induce tau phosphorylation and loss of microtubule binding. *Neuron* **14:** 879-888

Hoogenraad CC, Bradke F (2009) Control of neuronal polarity and plasticity--a renaissance for microtubules? *Trends in cell biology* **19:** 669-676

Kayed R, Head E, Thompson JL, McIntire TM, Milton SC, Cotman CW, Glabe CG (2003) Common structure of soluble amyloid oligomers implies common mechanism of pathogenesis. *Science (New York, NY* **300:** 486-489

Klein WL, Stine WB, Jr., Teplow DB (2004) Small assemblies of unmodified amyloid beta-protein are the proximate neurotoxin in Alzheimer's disease. *Neurobiology of aging* **25:** 569-580

Kuperstein I, Broersen K, Benilova I, Rozenski J, Jonckheere W, Debulpaep M, Vandersteen A, Segers-Nolten I, Van Der Werf K, Subramaniam V, Braeken D, Callewaert G, Bartic C, D'Hooge R, Martins IC, Rousseau F, Schymkowitz J, De Strooper B (2010) Neurotoxicity of Alzheimer's disease Abeta peptides is induced by small changes in the Abeta42 to Abeta40 ratio. *The EMBO journal* **29:** 3408-3420

Lacor PN, Buniel MC, Chang L, Fernandez SJ, Gong Y, Viola KL, Lambert MP, Velasco PT, Bigio EH, Finch CE, Krafft GA, Klein WL (2004) Synaptic targeting by Alzheimer's-related amyloid beta oligomers. *J Neurosci* **24:** 10191-10200

Lopez del Amo JM, Schmidt M, Fink U, Dasari M, Fandrich M, Reif B (2012) An asymmetric dimer as the basic subunit in Alzheimer's disease amyloid beta fibrils. *Angew Chem Int Ed Engl* **51:** 6136-6139

Michaelis ML, Chen Y, Hill S, Reiff E, Georg G, Rice A, Audus K (2002) Amyloid peptide toxicity and microtubule-stabilizing drugs. *Journal of molecular neuroscience : MN* **19:** 101-105

O'Nuallain B, Freir DB, Nicoll AJ, Risse E, Ferguson N, Herron CE, Collinge J, Walsh DM (2010) Amyloid beta-protein dimers rapidly form stable synaptotoxic protofibrils. *J Neurosci* **30:** 14411-14419

Salinas S, Carazo-Salas RE, Proukakis C, Cooper JM, Weston AE, Schiavo G, Warner TT (2005) Human spastin has multiple microtubule-related functions. *Journal of neurochemistry* **95:** 1411-1420

Walsh DM, Selkoe DJ (2007) A beta oligomers - a decade of discovery. *Journal of neurochemistry* **101:** 1172-1184

Zempel H, Mandelkow EM (2012) Linking amyloid-beta and tau: amyloid-beta induced synaptic dysfunction via local wreckage of the neuronal cytoskeleton. *Neuro-degenerative diseases* **10:** 64-72

Zempel H, Thies E, Mandelkow E, Mandelkow EM (2010) Abeta oligomers cause localized Ca(2+) elevation, missorting of endogenous Tau into dendrites, Tau phosphorylation, and destruction of microtubules and spines. *J Neurosci* **30:** 11938-11950

Figure S1 , *Zempel et al.*

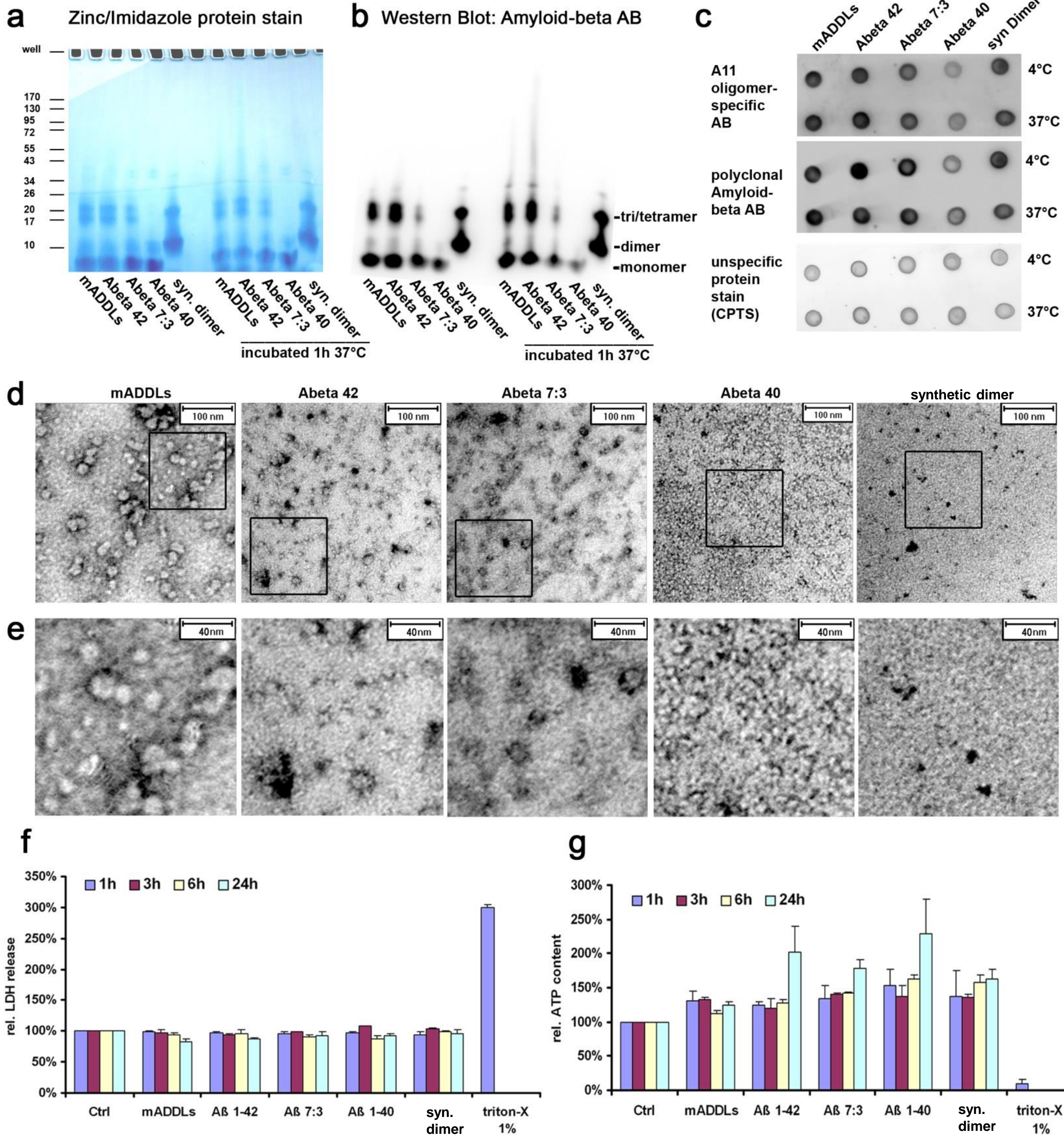

Figure S2 , *Zempel et al.*

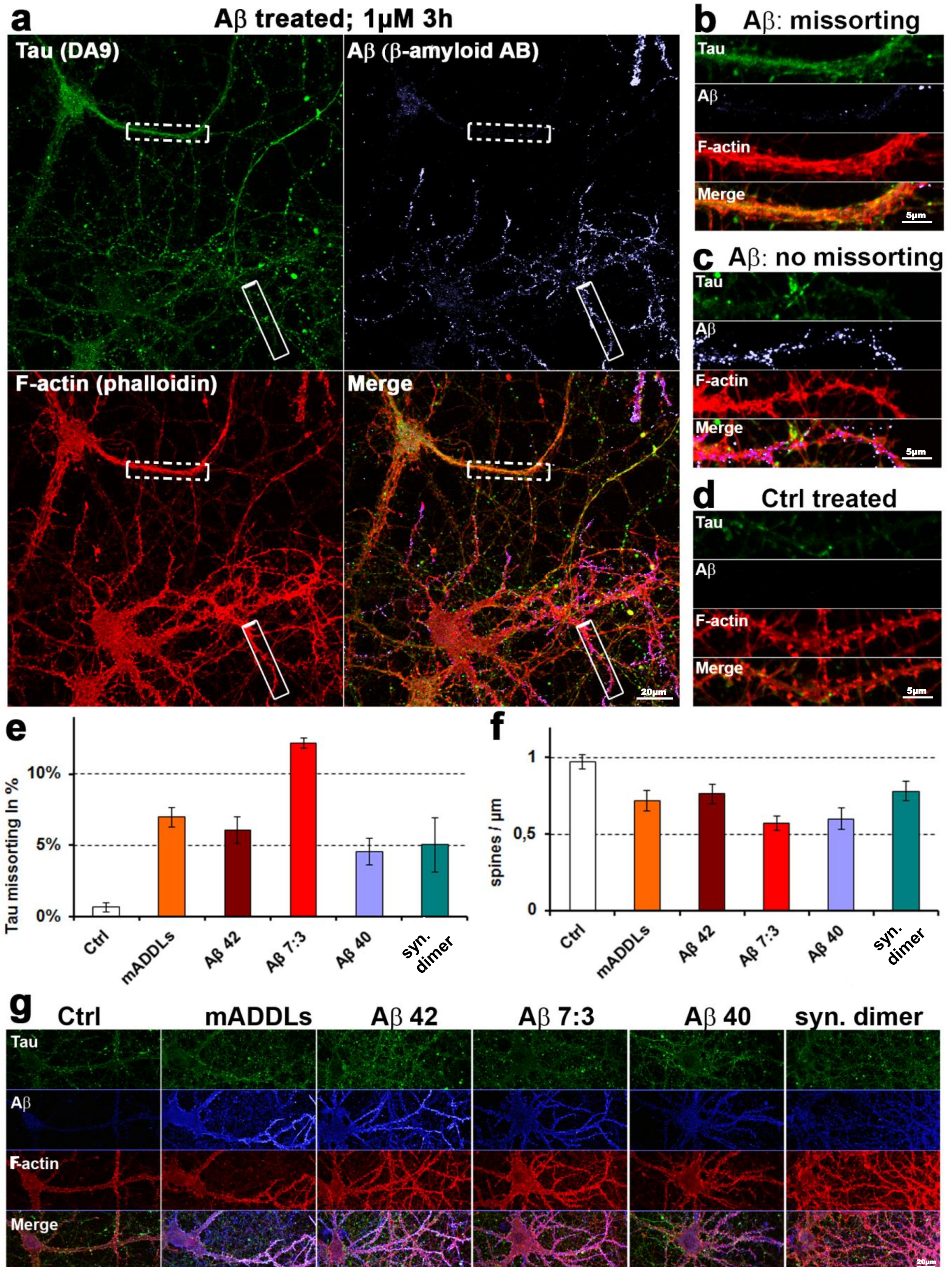

Figure S3, *Zempel et al.*

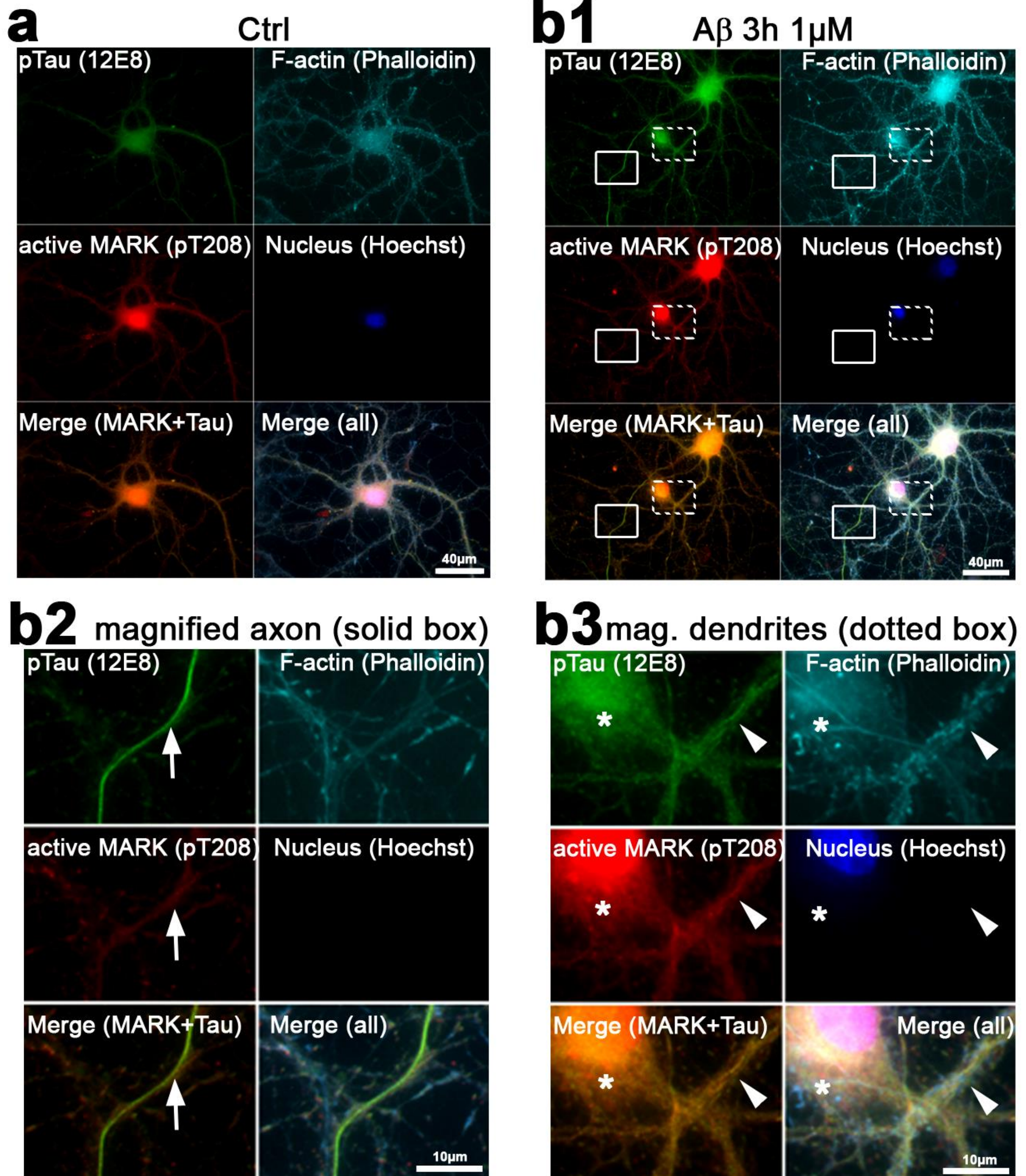

Figure S4 , *Zempel et al.*

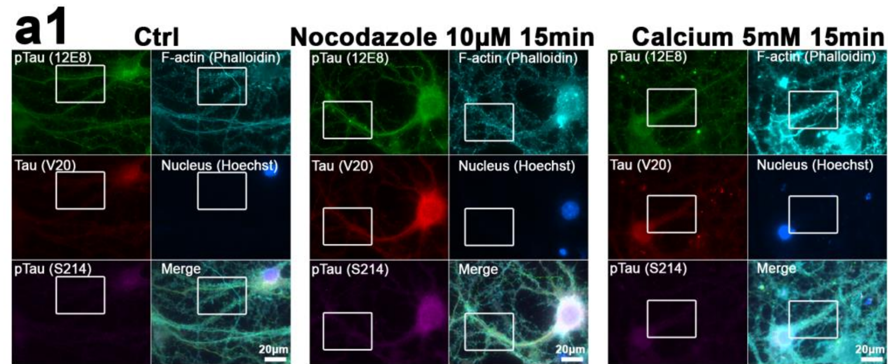

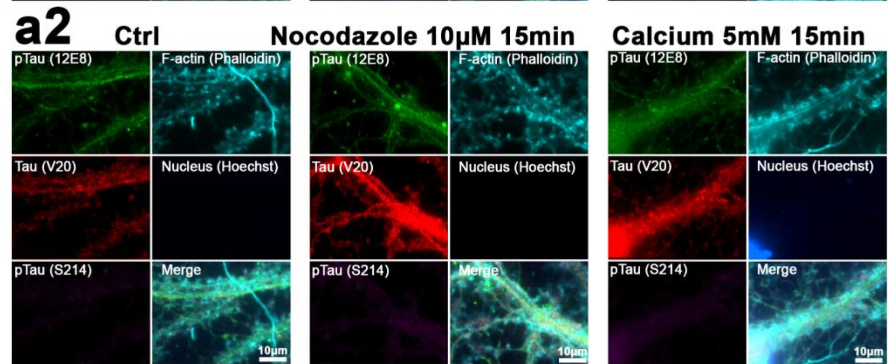

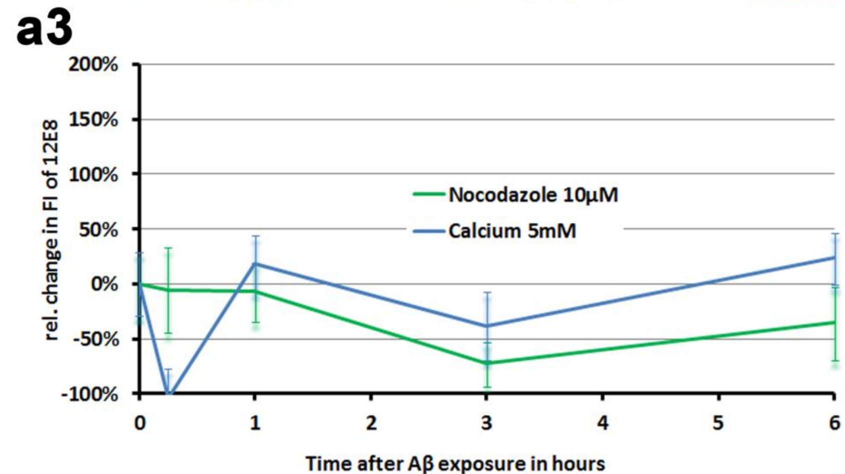

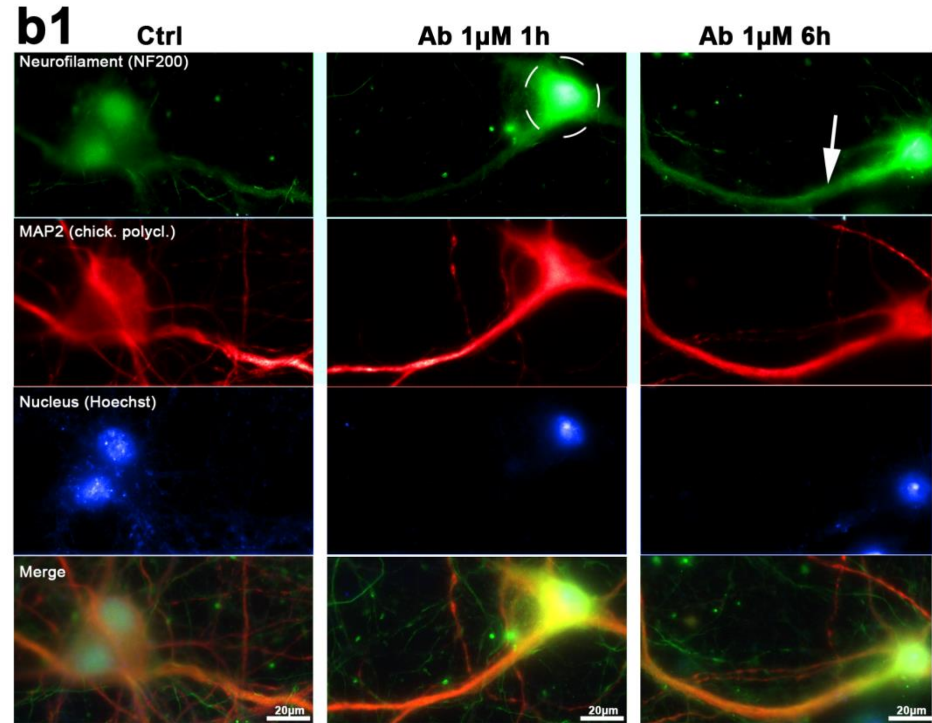

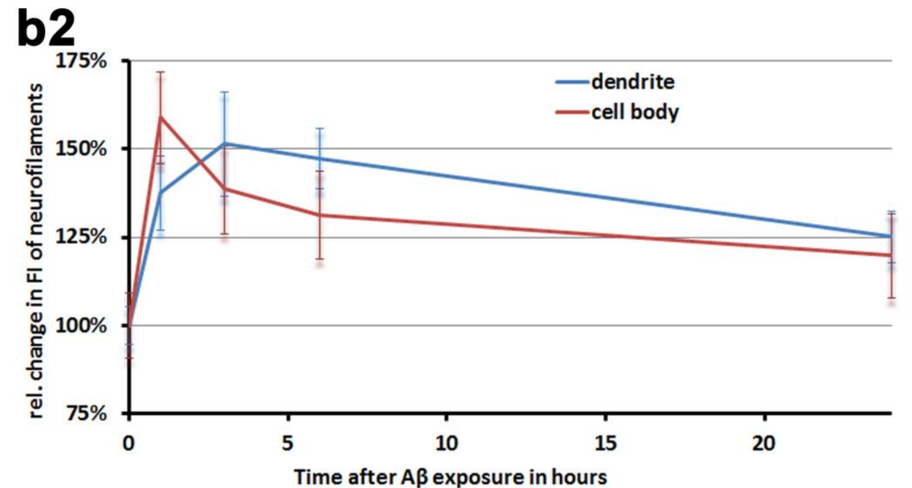

Figure S5, *Zempel et al.*

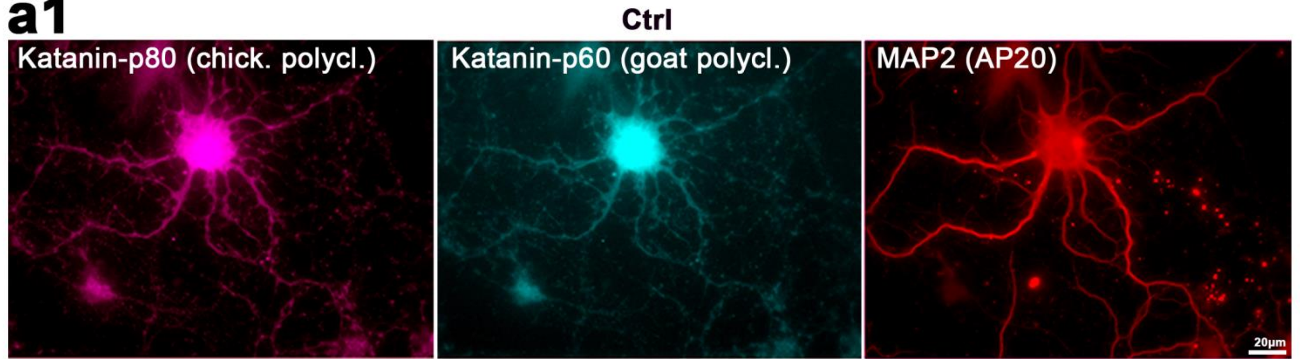

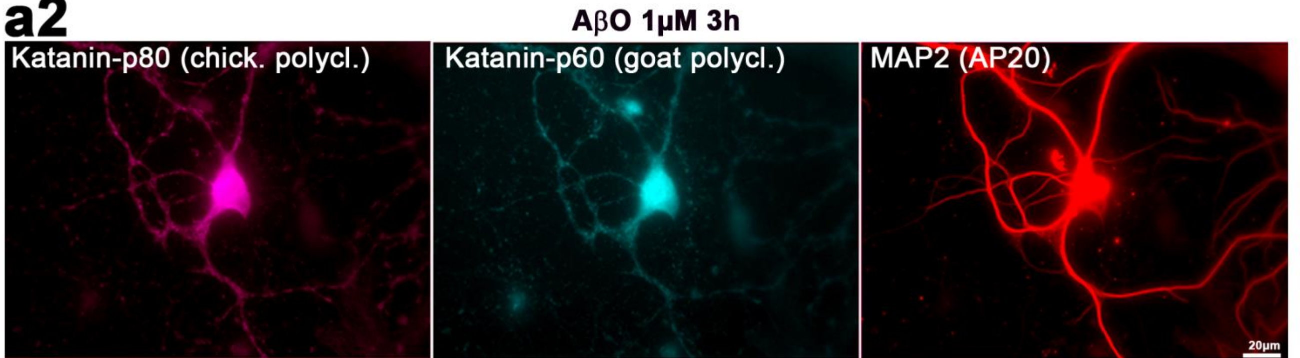

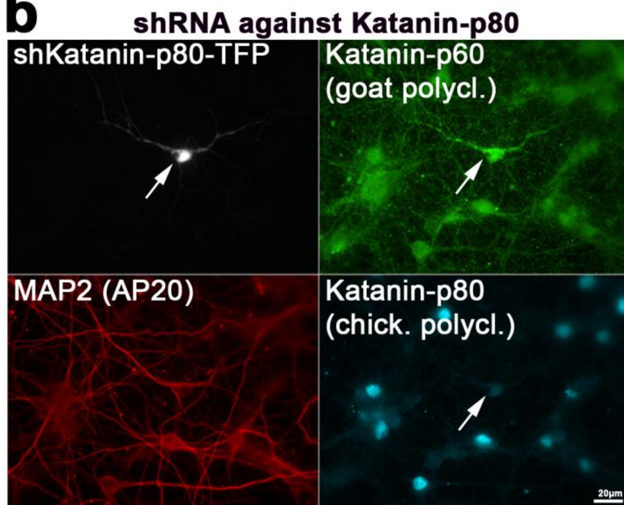

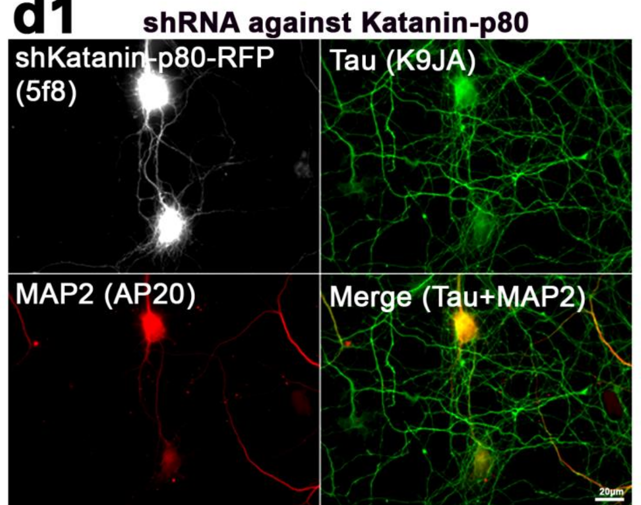

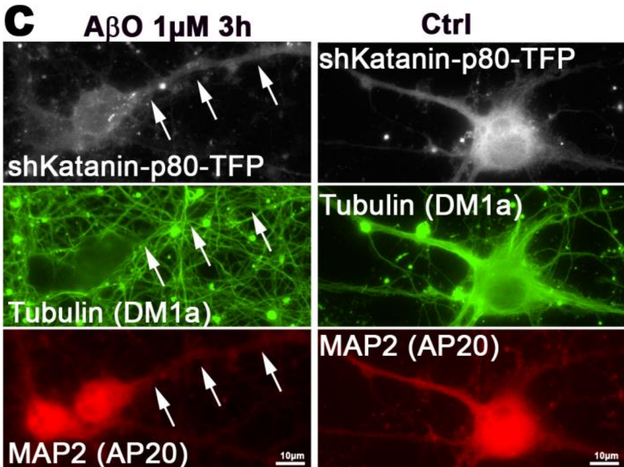

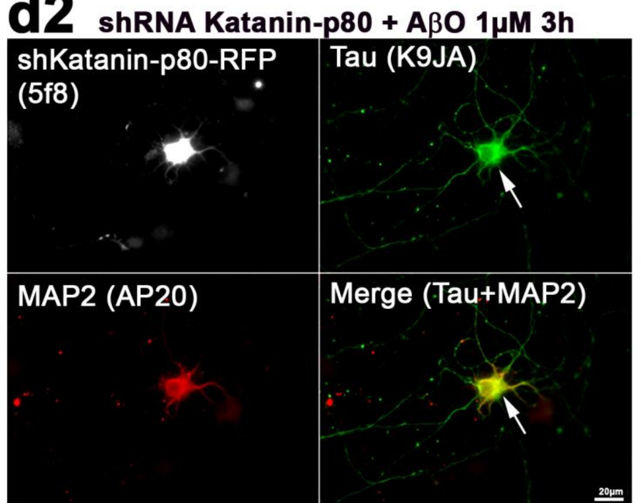

Figure S6 , *Zempel et al.*

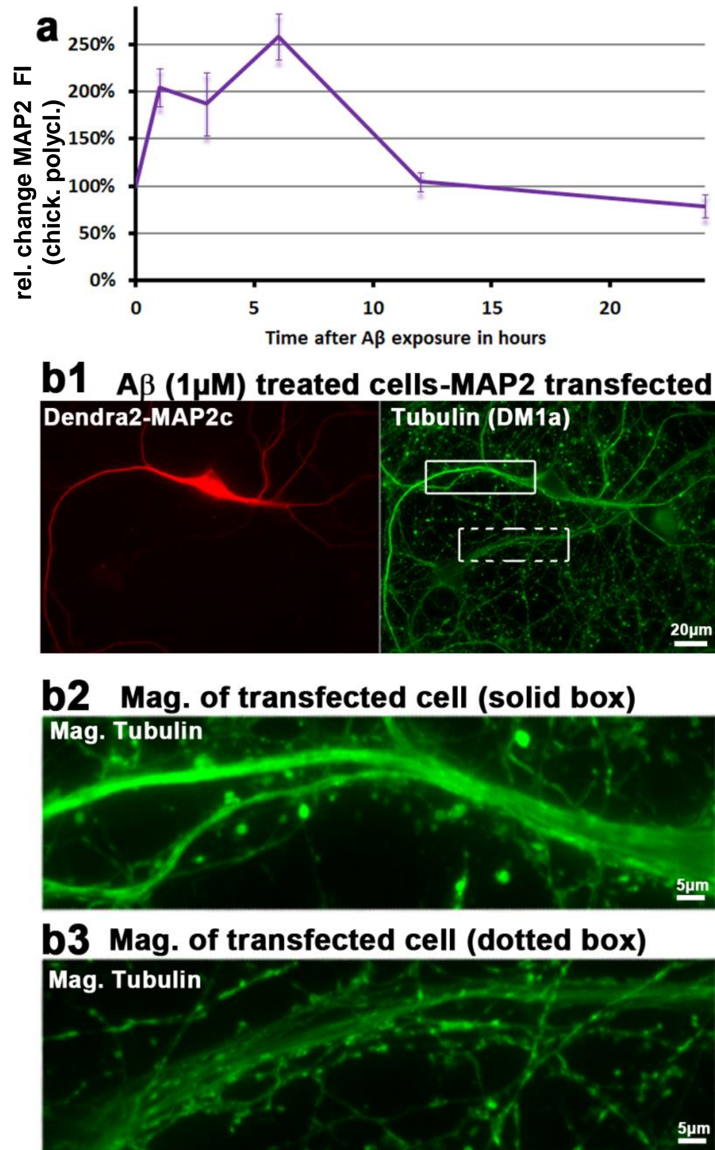

Figure S7 , *Zempel et al.*

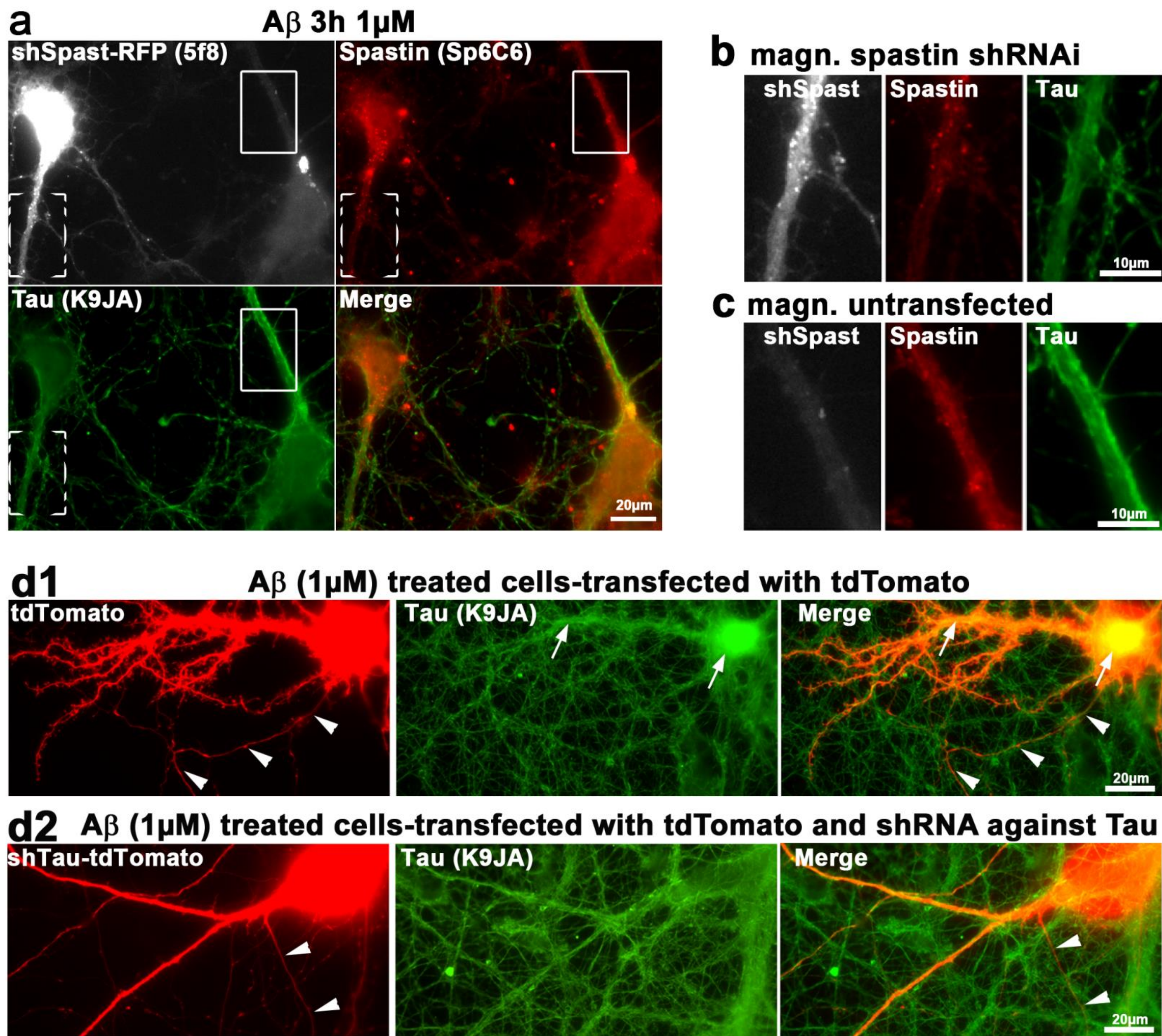

Figure S8, *Zempel et al.*

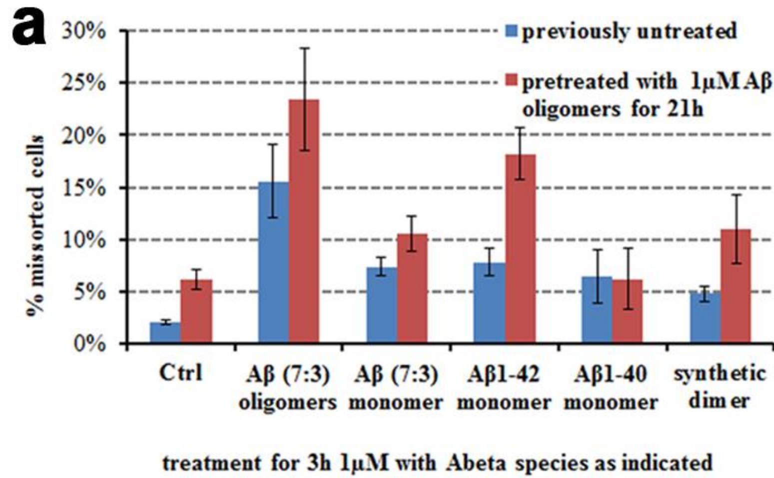

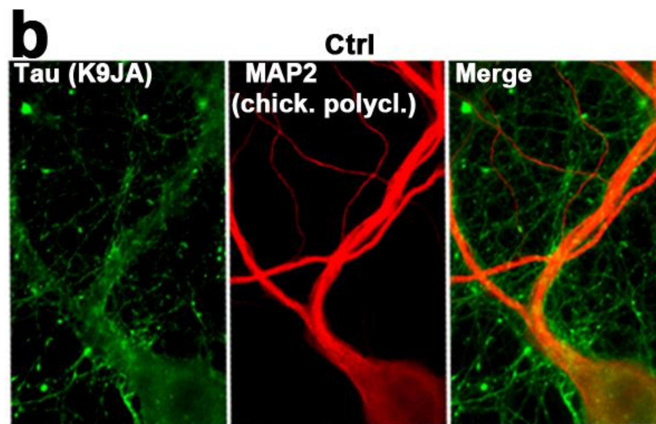

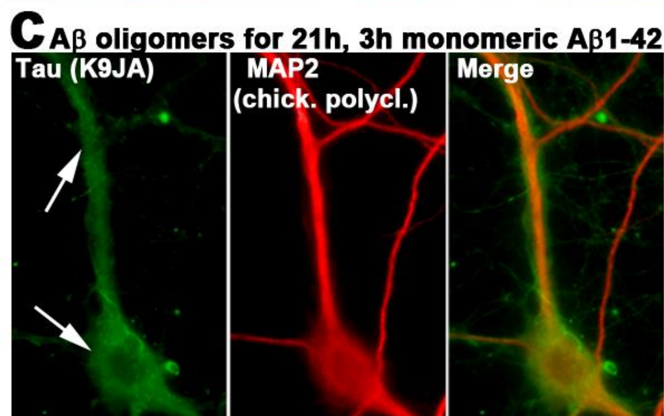

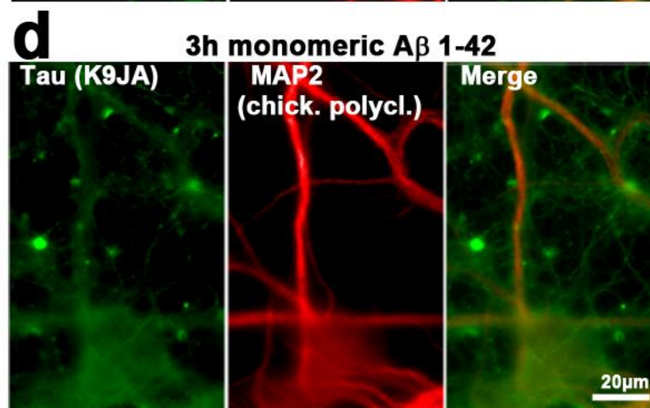

Figure S9, *Zempel et al.*

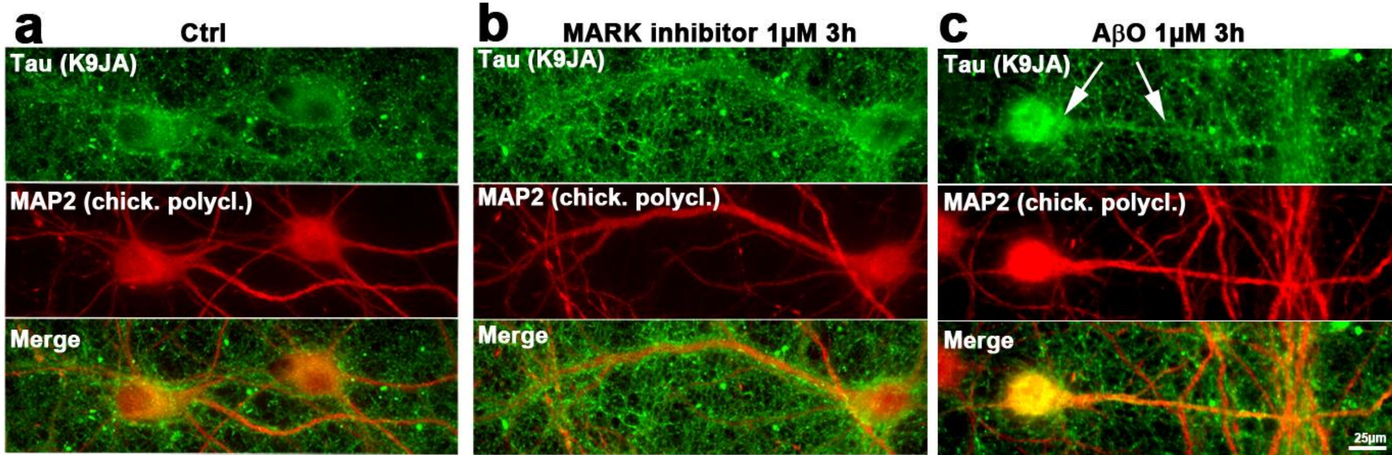

Figure S10, *Zempel et al.*

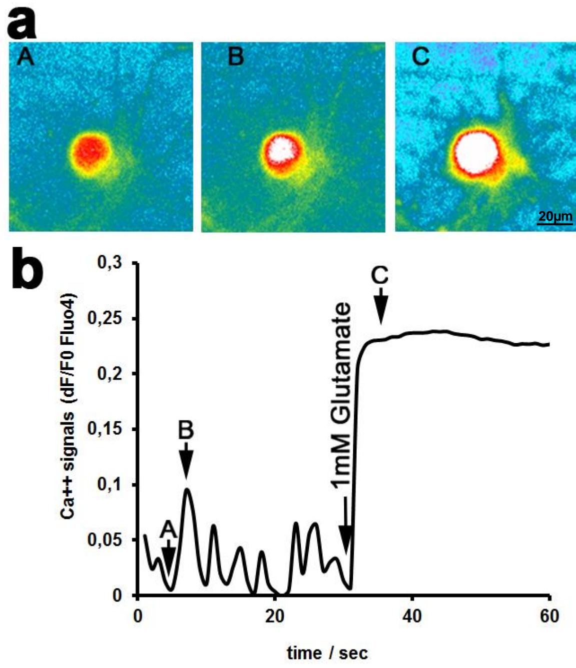

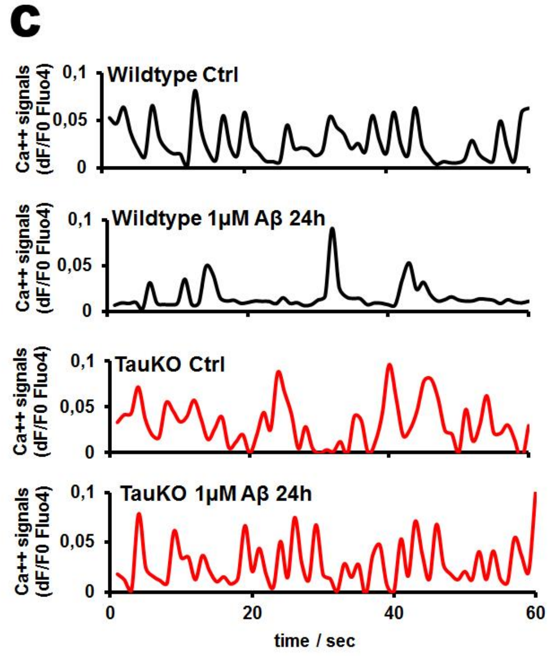

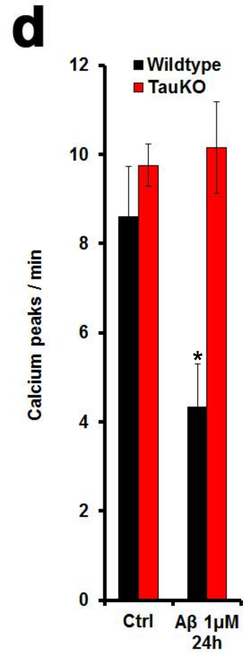

Figure S11, *Zempel et al.*

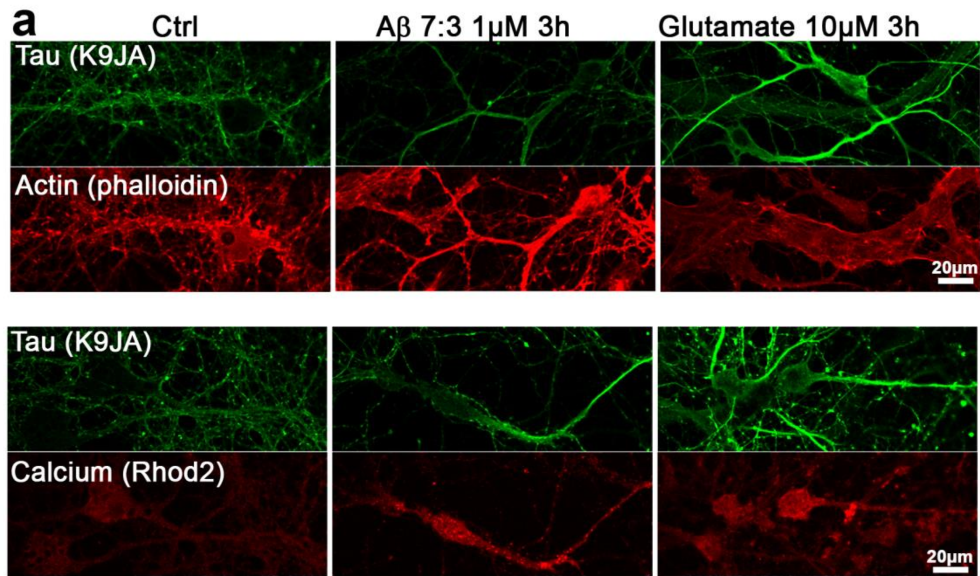

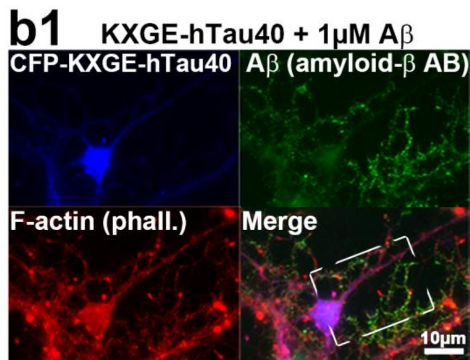

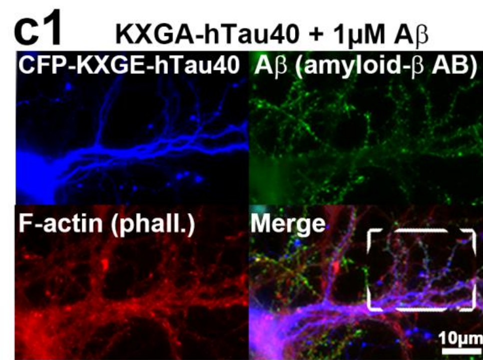

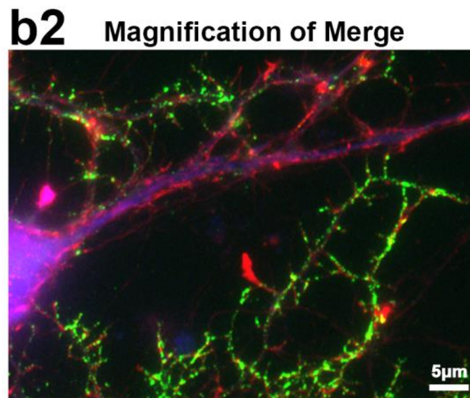

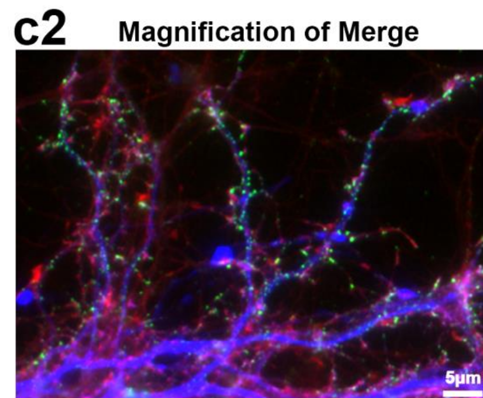

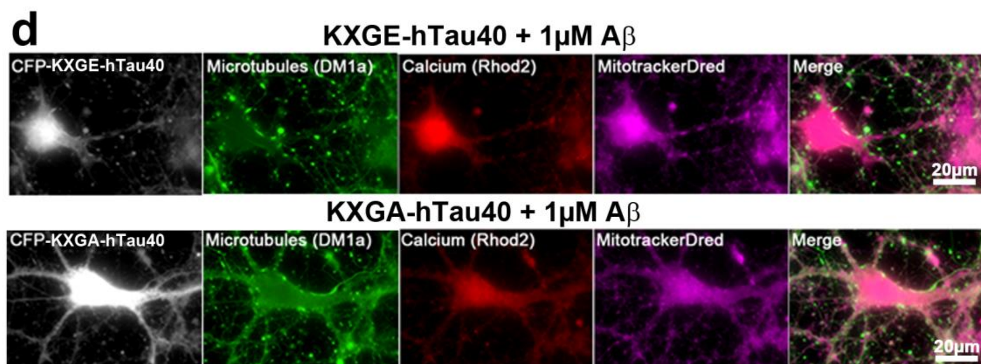

Figure S12, *Zempel et al.*